AIAA 91-1711

Investigation of Flow Field on a Hammerhead Nose Configuration at Transonic Speeds

S. Ahmed and S.Selvarajan
National Aeronautical Laboratory
Bangalore, INDIA

AIAA 22nd Fluid Dynamics, Plasma Dynamics & lasers Conference
June 24-26,1991 / Honolulu, Hawaii

Investigation of Flow Field on a Hammerhead Nose Configuration at Transonic Speeds

S.Ahmed [1]

and

S.Selvarajan

Experimental Aerodynamics Division
National Aeronautical Laboratory, Bangalore 560037, INDIA

Abstract

Flow field at transonic Mach numbers of a hammerhead nose configuration with boat tail angles in the range of 0 to 90 degrees is studied through surface flow visualisation and surface pressure measurements. Surface steady pressure data shows presence of a shock on the cylindrical portion of the body that shifts downstream with increase in Mach number and boat tail angle. Maximum travel of the shock wave is observed at boat tail angle of 90 degrees. Analysis of unsteady pressure data shows evidence of shock oscillations with multiple frequency content at M=0.9. Results of the tests on a scaled model in two different tunnels show that the oscillations are due to the nature of unsteadiness in the tunnel. Variation of the boat tail angle does not appear to alter the unsteadiness in the cylindrical region at transonic speeds.

Nomenclature

P	local static pressure
p_∞	free stream static pressure
p'	rms value of pressure fluctuations
q	free stream dynamic pressure
Δp	pressure fluctuations measured in a band of Δf = 0.72Hz, psi
f	frequency of pressure fluctuations, Hz
M	free stream Mach number
X	distance from the cone-cylinder junction
X_s	Shock position
D	maximum diameter of the model
θ	boat tail angle
C_p	steady pressure coefficient= $\frac{p-p_\infty}{q}$
C_{p*}	steady pressure coefficicent at local Mach number of 1.0
$C_{p'}$	unsteady pressure coefficient=$

1 *Research Scientist; MCAT Institute, San Jose, CA, Member AIAA. On Leave from National Aeronautical Laboratory, Bangalore, India. Mailing Address: M.S. 260-1. NASA Ames Research Center, Moffett Field, CA 94035*

1. Introduction

For missiles and launch configurations, bulbous nose shapes have become imperative from the consideration of accomodating larger pay loads. However, these configurations have ehown a tendency of becoming dynamically unstable at transonic speeds due to large negative damping associated with shock induced separation (ref.1). Analytical studies have been made by Ericsson to determine the aeroelastic response of a space vehicle caused by this type of shock induced flow separation (ref.2). However, a detailed investigation of the flow field on a bulbous nose configuration is lacking to fully understand the nature of flow field, particularly at transonic speeds. Cole et al (ref.3) have suggested certain geometric parameters for a hammerhead configuration to be buffett free. However, data available in the literature is not adequate to ascertain how these criteria have been specified. One of the important configuration parameters identified to be critical in terms of flow stability is the variation in the angle of the boat tailed body. This parameter is taken as a test parameter in the present paper and the steady and unsteady flow field are studied for a series of hammerhead configurations at transonic speeds. The data thus generated would be helpful in analysing the aeroelastic response of the configuration and in developing better CFD codes for understanding the physics of the flowfield. The investigations were carried out in the 1.2M trisonic wind tunnel of the National Aeronautical Laboratory, Bangalore, India.

2. Facility description

1.2M trisonic wind tunnel is a blowdown type of tunnel operating in the Mach number range of 0.2 to 4.0. Transonic Mach numbers are attained in a separate test section of size 1.2M X 1.2M which has perforated walls on all the sides. The holes on the side wall are normal and having a open area ratio of 20 percent where as the top and bottom walls are inclined at 60 degrees, and have an open area ratio of 6 percent. Mach number in the test section is controlled by adjustable flaps located at the end of test section. Models are usually sting mounted and can be pitched from -15 to 27 degrees. The usual operating pressure of the tunnel is about 2 atmospheres

and the maximum operating pressure is about 6 atmospheres at supersonic Mach number of 4.0. The flow characterisitics of the tunnel are shown in fig.1

3. Model Details

The geometric details of the model are shown in fig.2. The model consists of a 20 degrees ball nosed cone followed by a cylindrical portion and variable boat tailed body, ending in a long cylindrical portion. The model has mechanical provision to fix boat tailed bodies of various angles of upto 90 degrees. Measurements are restricted to the cylindrical portion and to the two generators located at 90 degrees interval apart. Static taps on one of the generators are located at 5mm interval and these are in turn connected to a scanivalve (with a ± 10 psid transducer) housed inside the model. On the other generator, 5 Kulite transducers (± 5psid) of 6.35mm dia are located very close to the surface of the model through a cavity at X/D = -0.15, 0.07, 0.24, 0.41, 0.59 and 0.75. The response of the cavity was measured in an acoustic test facility and the frequency response was flat upto 2KHz. Spatial location of the transducers was determined by the size of transducer and the mounting arrangement. The natural frequency of the model along with its supporting system is about 30 Hz.

4. Test Conditions

Both steady and unsteady pressures on the surface were recorded at nominal Mach numbers of 0.8, 0.85, 0.9, and 0.95, at the model incidence of zero degree. The boat tail angle of the model was varied at 0, 5, 15, 30, 45, 60, 90 degrees. The Reynolds number(based on the maximmum diameter of the model) variation was from 3.5 to 3.8 million in the Mach number range tested.

5. Instrumentation

Electrical leads from the transducer and the scanivalve were brought out of the test section and connected to Preston amplifiers located close to the tunnel. Length of the leads was kept to a minimum to keep the noise of the system low and to get a higher signal to noise ratio. Amplifier gain settings were varied depending on the transducer type and its location in the flow field. Filter setting on the amplifier was kept constant at 10 KHz. Analog signals from the amplifiers were recorded on a 16 channel Honeywell tape recorder. As the facility is a blowdown type and the duration of flow is restricted, the signals were recorded for about 30 seconds. Signal from each of the transducer was fed through a DISA rms meter to obtain the root mean square value of the signal and through a DISA spectrum analyser to obtain the frequency spectrum. Spectral analysis of the signal was carried out for two ranges of frequencies viz., 0 to 200Hz and 0 to 10KHz. The low range frequency analysis was done to investigate the presence of any low frequency component of the signal, which may excite the model/launch vehicle frequency and high range frequency spectrum was utilised to ascertain the total unsteady content of the signal. During analysis the DC level of the signal was also noted to check and compare the steady pressure data obtained on the other generator.

6. Results and Discussion

6.1 Steady pressures

6.1.1 Effect of Mach number at $\theta = 15^0$

Steady pressue data obtained on the surface of the model for the boat tail angle of 15 degrees in the test Mach number range is shown in fig.3. C_{p*} corresponding to the free stream Mach number is also marked for each curve. The data shows strong acceleration of the flow to supersonic speeds at the cone cylindrical junction as evidenced by the strong suction peak, and deceleration of flow to free stream conditions on the cylindrical region. At M=0.8, as the flow decelerates from supersonic Mach number a change in the pressure gradient can be seen at X/D=0.15 at C_p close to C_{p*}. This is due to deceleration of flow from a weak shock wave or through a series of compression waves. For the next higher Mach number of 0.85, a change of pressure gradient occurs at X/D=0.2 and the pressure variation is similar to what occurs in a shock boundary layer interaction region (ref.4), indicating the presence of a strong shock near this location. For higher Mach numbers, the data shows that the point at which the abrupt change in pressure occurs shifts downstream indicating a corresponding downstream shift of the shock wave. It can also be seen from the figure that the supersonic region grows with increase in Mach number.

6.1.2 Effect of Mach number at $\theta = 90^0$

Fig.4 shows the pressure variation on the cylindrical region with Mach number. These curves exhibit similar variation with X/D as in fig.3. For M=0.8, at X/D=0.1 the C_p value is about -0.9 and in contrast to -1.2, the value for $\theta = 15^0$ case. This indicates that the flow accelerates to a higher Mach number for lower boat tail angle. At M=0.85, the abrupt change in the pressure gradient occurs at X/D=0.2 for $\theta = 15^0$ and corresponding value for $\theta = 90^0$ is X/D=0.17. Also the farthest position of the shock is at X/D=0.7 and corresponding location for $\theta = 15^0$ is X/D=0.8. It is difficult to conclude whether the shift in shock observed is due to a variation in boat tail angle. Shift of shock position with Mach number is discussed in the following section.

6.1.3 Effect of Boat tail at M = 0.89

Fig.5 shows the effect of boat tail angle on the C_p variation at M=0.89. Here the pressure data is compared with a cone cylinder body. C_p's shown are for boat tail bodies of 30 and 90 degrees. For $\theta = 0^0$, a change in the gradient of pressure occurs at X/D=0.3 and at C_p=-0.90. The corresponding values for $\theta = 30^0$

and 90^0 are 0.45 and 0.40 respectively. Though a distinct shift is observed for the cone cylinder body with a lower boat tail angle, it is not clear whether the shift of X/D = 0.05 observed is due to a variation in boat tail angle. It is possible that the shift seen may be due to the free stream Mach number being not same and the shock position may be sensitive to a small increment in the Mach number. Shock position as observed by a change in the pressure gradient/an abrupt increase in pressure from the pressure distribution curve is plotted as a function of Mach number and is shown in fig.6, for two cases namely $\theta = 0^0$ and $\theta = 90^0$. It can be seen from the figure that the shock position has shifted downstream for the boat tailed body and also the travel of the shock wave in the Mach number range of 0.84 to 0.91 is about 0.55 for a boat tailed body compared to 0.44 for a cone cylinder body. This indicates that the travel of the shock wave is larger for a boat tailed body.

6.2. Unsteady Pressures

Initially unsteady pressures were measured on a cone cylinder body with a boat tail angle of 5 degrees. Results of these measurements are shown in figures 6 and 7 for Mach numbers of 0.8 and 0.92 respectively. Unsteady pressure data is represented in terms of root mean square values ($C_{p'}$) and the frequency spectrum (Ap) where Δp is the pressure fluctuation in a constant band width of 0.72Hz at a center frequency f. To get an understanding of the flow physics, surface flow patterns in the region of measurements were obtained using standard mixture of titanium di oxide, oelic acid and engine oil in approriate proportion and these are shown in the figures 7 and 8.

6.2.1 Unsteady Pressures at M=0.8

Unsteady pressure history at M=0.8 is shown in fig.7. Surface flow pattern (fig.7a) shows separation at the corner in the form of a bubble. This separation is due to the adverse pressure gradient from the compression waves and exhibits characteristics of separation at an expansion corner. Spectrum of the unsteady signal (fig.7b) at X/D=-0.15 shows no significant content of pressure fluctuations in the range of frequency shown. The level of pressures is expected to be low at this location due to the boundary layer. The range of spectrum is restricted to 200Hz as the interest is to observe the existence of low frequencies. At X/D= 0.24 (fig.7c) which is inside the bubble and close to the reattachment region, the level of pressure fluctuation is higher in the frequency range of 0 to 100Hz. This is expected of a separated flow. Spectrum of the signal at X/D=0.59 (fig.7d) shows the level of pressure fluctuation recovering to free stream value as in fig.7b. The dominant frequency seen at 115Hz in the spectra shown is due to the free stream noise . This is confirmed by side wall pressure measurement.

The total unsteadiness of the signal along with the static pressure data is shown in fig.7e. Maximum $C_{p'}$ is seen around X/D=0.2, where the flow reattaches to the surface and the unsteadiness can be seen to be recovering to the free stream value at X/D=0.75. The corresponding static pressures from the unsteady signal are also shown. At least in the region of subsonic flow the rms values appear to be dependent on the local static pressure.

6.2.2 Unsteady pressures at M=0.92

Fig.8 shows the variation of unsteady pressures at M=0.92. Surface flow pattern at M=0.90 is shown for reference (fig.8a). Spectrum at X/D=0.24 (fig.8b) shows low content of unsteadiness similar to that at M=0.8 (fig.7b), whereas the spectrum at X/D=0.59 (fig.8c) shows dominant spikes at 38Hz, 65Hz, and 100Hz. Steady pressures (fig.8d) show an abrupt increase in pressure due to the presence of the shock and also the rms value of the signal increases. The presence of dominant spikes indicate that the shock is oscillating at multiple frequencies. Shock oscillations due to model support system is not expected at these frequencies, as the natural frequency of the model and its support system is about 30Hz, and the free stream unsteadiness shows dominant frequency at 120Hz. Shock oscillations at multiple frequencies are observed on an airfoil by Finke (ref.5) and on curved channels by Meier (ref.6) at transonic speeds. It is reasoned initially that these oscillations might be due to the interaction of shock with the boundary layer causing it to separate and the separated flow then interacting with the flow in the boat tail region triggering the oscillation of the shock wave.

6.2.3 Measurements on a scaled model

To confirm the existence of shock oscillations at transonic speeds, experiments were conducted on a scaled model of diameter 43.75mm dia and unsteady pressure data was obtained by testing the model in 0.3M transonic tunnel and 1.2Mtunnel. Kulite transducers of range ± 5psid transducer and dia 1.57mm were embedded inside the model with a cavity. The frequency response of the cavity was measured and found to be flat in the range of 0 to 5KHz. The 0.3M transonic tunnel is also a blow down tunnel with a test section size of 0.3M X 0.3M. Top and bottom walls of the test section are slotted while the side walls are solid. As the geometry of the wall of the test section is differrent it is expected to have a different flow characteristics at the transonic speeds compared to that seen in the 1.2M tunnel.

Spectral data at the location X/D=0.74 at M=0.9 is shown in fig.9a. The corresponding free stream spectrum measured at the side wall of the tunnel is also shown (fig.9b). The spectrum obtained is different from that shown in fig.8c and no dominant spikes can be seen. Maximum pressure fluctuation are seen in the frequency range of 80 to 140Hz and the side wall spectra show maximum pressure fluctuations in the range of 120 to 180Hz. As the model frequency of vibration is about 95Hz it is difficult to conclude if the oscillations were triggered by the model vibration as the spectrum appears to be spread over a frequency band.

Frequency spectrum of the unsteady pressures at X/D=0.74 (fig.9c) of the same model obtained through tests in the 1.2M tunnel shows spectrum characteristics identical to that shown in fig.8c. As the scale of the model is varied, it is expected that the frequency of the shock oscillations will vary. The invariance of the frequency of shock oscillations with the scale of the model suggests that these oscillations are not due to the flow, but due to the unsteadiness present in the tunnel. Sources of unsteadiness in the tunnel has to be investigated to find the cause for the occurence of these oscillations.

6.2.4 Effect of Boat tail angle on Unsteadiness

Fig.10 shows the spectra of pressure fluctuations at M=0.9 at X/D=0.4 for the cone cylinder body with a boat tail angle of 15 degrees and 90 degrees. These spectra are nearly identical with the spectrum shown in fig.8c and there is no variation in the frequency of shock oscillations due to a change in the boat tail angle. This suggests that even though the shock induced separated flow interacts with the flow on the boat tailed body, the shock oscillations are not triggered by this interaction.

Oil flow pattern presented in fig.8a shows no accumulation of oil as the shock is oscillating. It is possible to misinterpret this pattern as formed by a weak shock wave in the absence of unsteady pressure measurements.

7. Conclusions

Surface flow field of cone cylinder boat tailed bodies with boat tail angles varying from 0 to 90 degrees is investigated at transonic Mach numbers and at zero degree incidence. Results of this study indicate the following:

1. Presence of shock in the cylindrical region and the shock moves downstream with increase in Mach number and with boat tail angle.

2. Maximum shift in the shock position is observed for a boat tailed body of 90 degrees.

3. Unsteady pressures show the presence of shock oscillations at M=0.92 for a boat tailed body of 5 degrees. Results of the study on a scaled model show the oscillations are due to the unsteadiness in the tunnel.

4. Frequency of shock wave oscillations remained invariant with the variation in the boat tail angle upto 90 degrees, for M=0.9.

5. The study suggests that the variation in the boat tail angle do not induce any additional low frequency unsteadiness in the cylindrical region.

8. Acknowledgements

Authors are thankful to the staff of model shop, 0.3M tunnel and 1.2 M tunnel for their assistance during the course of work.

9. References

[1] Cole, H.Jr, and Cue, C.F., "Dynamic Response of Hammerhead Launch Vehicles to Transonic Buffetting", NASA T N D 1982.

[2] Ericsson, L.E., "Aeroelastic Instability caused by Slender Pay Loads", Journal of Space Craft and Rockets", January 1967.

[3] Cole, H.A., Erickson, A.L., and Rainey, A.G., "Buffetting During Atmospheric Ascent, Space Vehicle Design Criteria", NASA SP 8001, November 1970.

[4] Chang, P.K., "Separation of Flow", Chapter 6, Pergamon Press, 1970.

[5] Finke, K., "Unsteady Shock Wave Boundary Layer Interaction on Profiles in Transonic Flow', AGARD CP 168, May 1975.

[6] Meier, G.E.A., "Shock Induced Flow Oscillations", AGARD CP 168, May 1975.

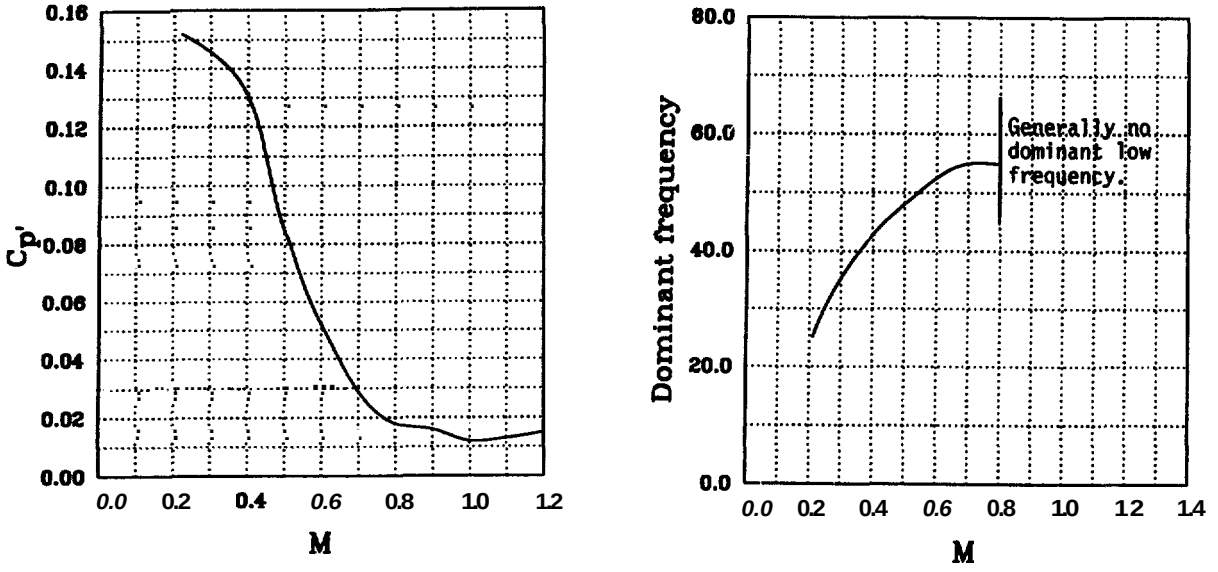

Fig.1 Flow Characterisitics of 1.2M Trisonic Wind Tunnel

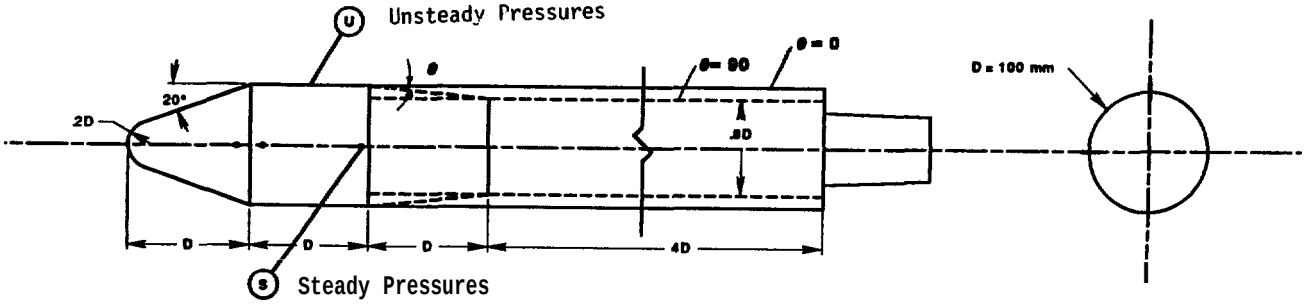

Fig.2 Geometrical Details of the Model

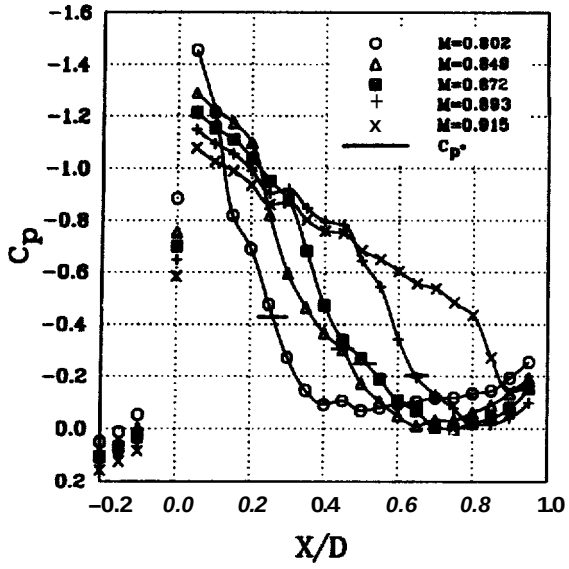

Fig.3 C_p Distribution at $\theta = 15^0$

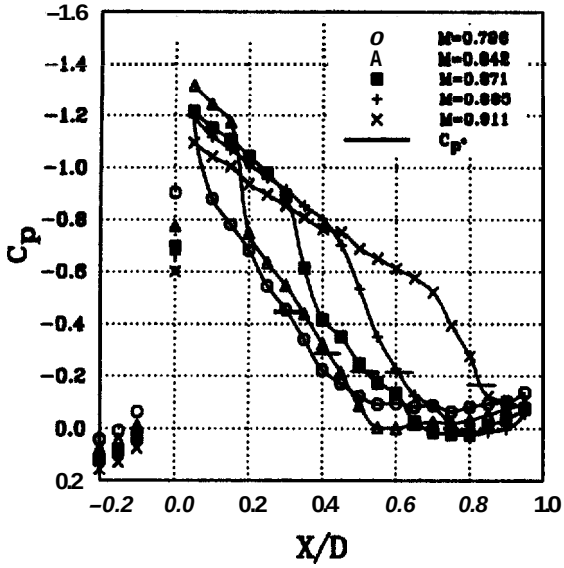

Fig.4 C_p Distribution at $\theta = 90^0$

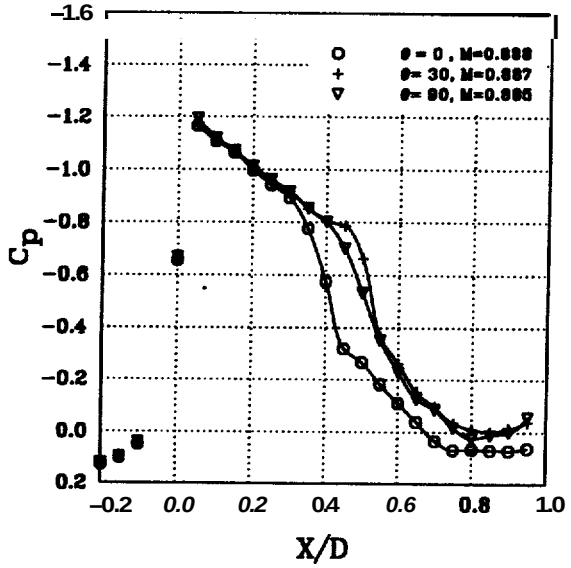

Fig.5 Effect of Boat Tail Angle at M = 0.89

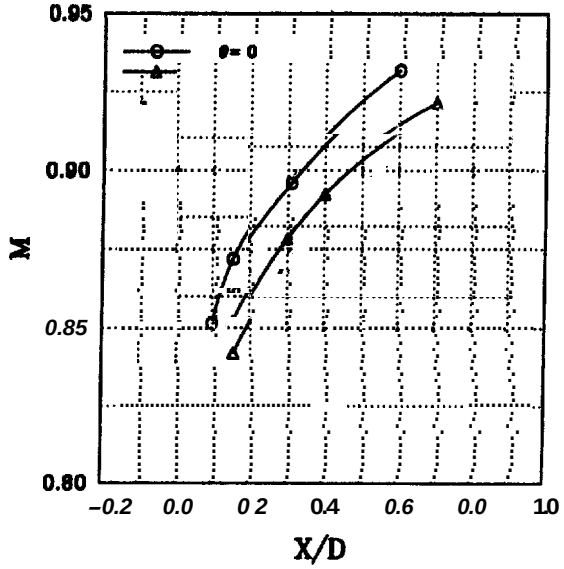

Fig.6 Effect of Boat Tail Angle on Shock Position

Fig.7a Surface Flow Pattern at M = 0.8

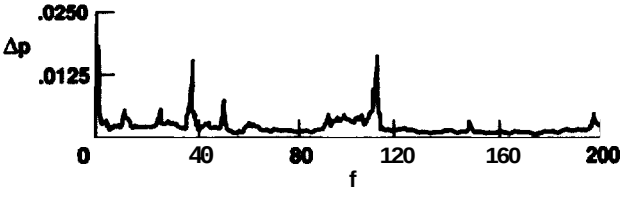

Fig.7b Spectrum Of Pressure Fluctuations at X/D= -0.15, M = 0.80

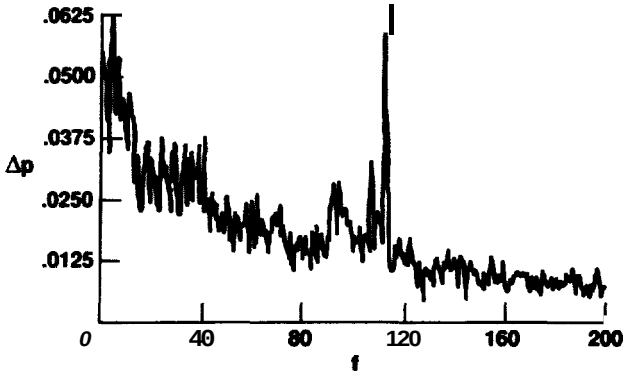

Fig.7c Spectrum of Pressure Fluctuations at X/D = 0.24, M = 0.80

Fig.7d Spectrum of Pressure Fluctuations at X/D = 0.59, M = 0.80

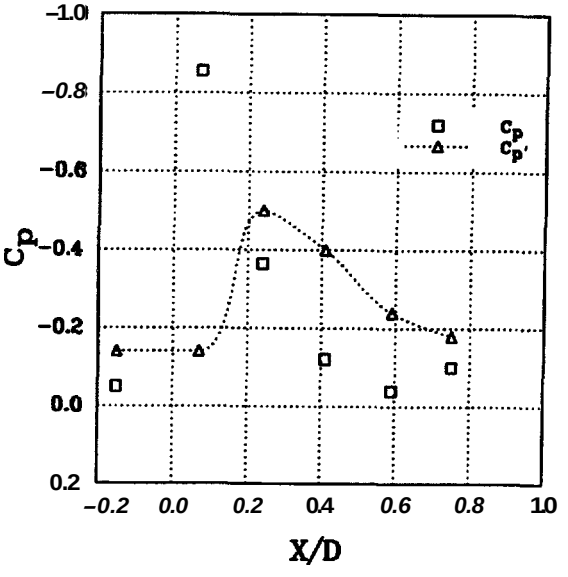

Fig.7e Variation of Unsteady Pressure Coefficient at M = 0.80, $C_{p'} = 0.1|C_p|$

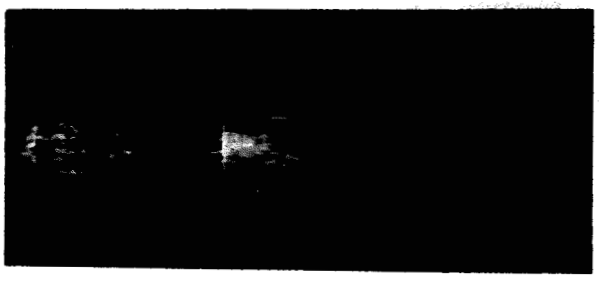

Fig.8a *Surface* Flow Pattern at M = 0.90

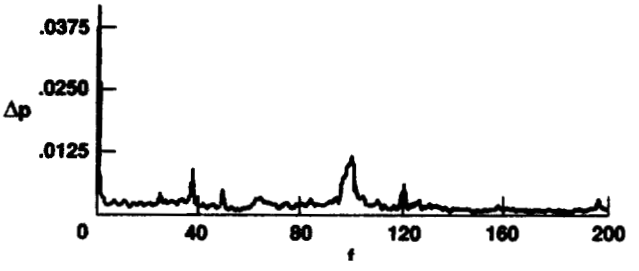

Fig.8b Spectrum of Pressure Fluctuations at X/D = 0.24, M = 0.92

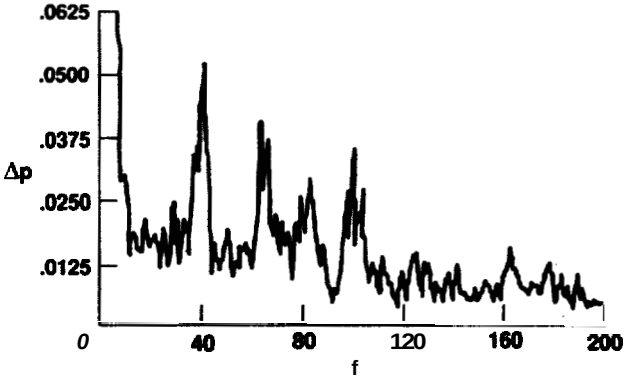

Fig.8c Spectrum of Pressure Fluctuations at X/D = 0.59, M = 0.92

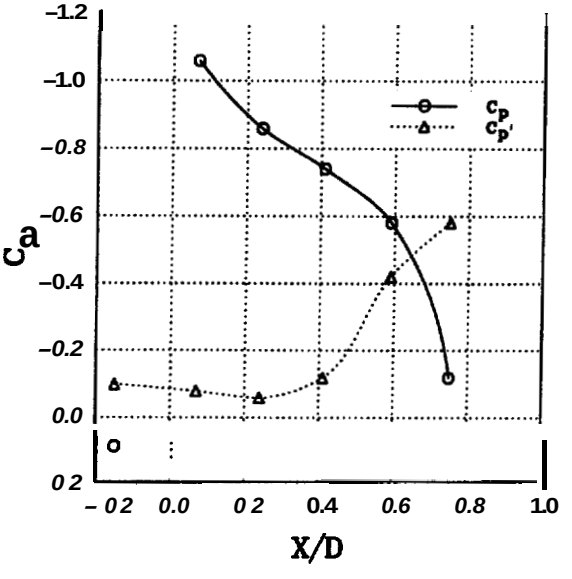

Fig.8d Variation of Unsteady Pressure Coefficient at M = 0.92, $C_{p'} = 0.1|C_p|$

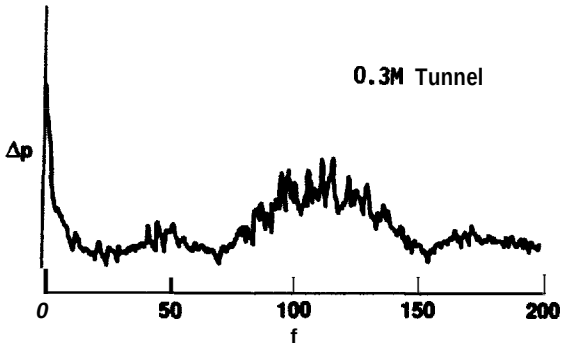

Fig.9a Spectrum of Pressure Fluctuations at X/D = 0.74, M = 0.92

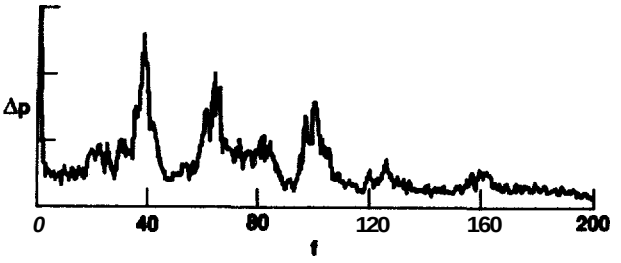

Fig.10a Spectrum of Pressure Fluctuations at X/D = 0.59, M = 0.92, $\delta = 15^0$

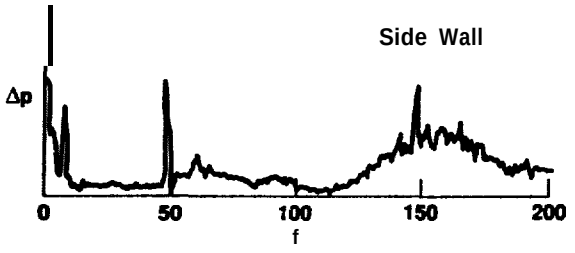

Fig.9b Spectrum of Pressure Fluctuations at M = 0.92, Side Wall

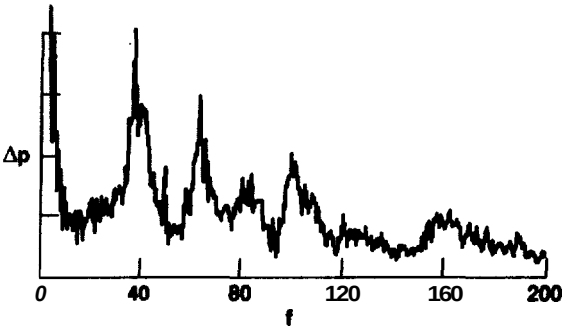

Fig.10b Spectrum of Pressure Fluctuations at X/D = 0.59, M = 0.92, $\delta = 90^0$

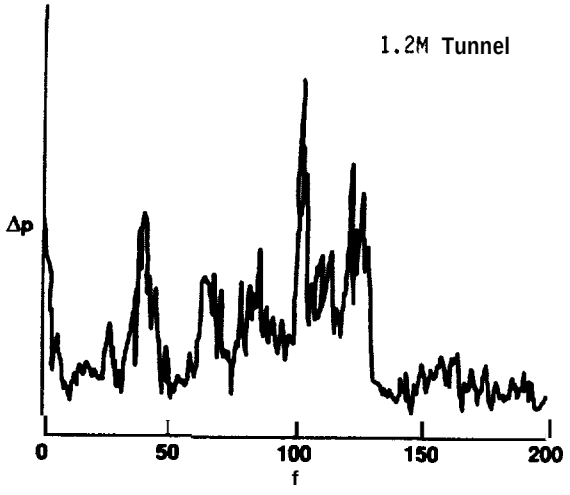

Fig.9c Spectrum of Pressure Fluctuations at X/D = 0.74, M = 0.92

AIAA 91-1711

Investigation of Flow Field on a Hammerhead Nose Configuration at Transonic Speeds

S. Ahmed and S.Selvarajan
National Aeronautical Laboratory
Bangalore, INDIA

AIAA 22nd Fluid Dynamics, Plasma Dynamics & lasers Conference
June 24-26,1991 / Honolulu, Hawaii